Large-scale neural network in passive silicon photonics for biologically plausible learning.

Alessio Lugnan[a], Alessandro Foradori[b,a], Stefano Biasi[a], Peter Bienstman[b], and Lorenzo Pavesi[a]

[a]Nanoscience Laboratory, Department of Physics, University of Trento, Italy
[b]Photonics Research Group, Ghent University - imec, Ghent 9052, Belgium

ABSTRACT

Neuromorphic computing hardware that requires conventional training procedures based on backpropagation is difficult to scale, because of the need for full observability of network states and for programmability of network parameters. Therefore, the search for hardware-friendly and biologically-plausible learning schemes, and suitable platforms, is pivotal for the future developments of the field. We present a novel experimental study of a photonic integrated neural network featuring rich recurrent nonlinear dynamics and both short- and long-term plasticity. Scalability in these architectures is greatly enhanced by the capability to process input and to generate output that are encoded concurrently in the temporal, spatial and wavelength domains. Moreover, we discuss a novel biologically-plausible, backpropagation-free and hardware-friendly learning procedure based on our neuromorphic hardware.

Keywords: Neuromorphic computing, machine learning, silicon photonics, reservoir computing, biologically plausible learning.

1. INTRODUCTION

Neuromorphic photonics, i.e. the realization of photonic artificial neural networks (ANNs), has recently shown great promise in overcoming important limitations of neuromorphic electronics.[1–3] Indeed, photonics allows for enhanced parallelism (e.g. via WDM techniques, short for wavelength division multiplexing) lower power consumption (no Joule heating) and reduced latency (e.g., no parasitic effects). However, training photonic neuromorphic hardware via conventional training algorithms based on backpropagation (BP) greatly limits the scalability of deployable networks and it is not a biologically plausible.[4,5] These limitations mainly arise from the requirements of observability and control of the network internal states and parameters, which are usually necessary to run BP.

In this work we investigate the employment of a photonic integrated ANN able to host complex and recurrent dynamics and to process information by exploiting the spatial, temporal and wavelength dimensions in parallel. The presented photonic ANN is very compact and simple to fabricate. It consists of 64 silicon microring resonators (MRRs, see Fig. 1 a), all coupled together by straight waveguides that are in turn connected to multiple input and output optical ports. Thanks to the complex dynamics enabled by silicon nonlinear effects and to the periodic resonances in a MRR spectrum,[6–8] the actual network is much larger than its spatial arrangement, as it is expanded through the temporal and wavelength domains, while preserving a small on-chip footprint. We show that several nonlinear representations of the input optical time series (flattened images from the MNIST dataset[9]) can be obtained in parallel at different wavelengths. These representations can be employed by a computationally cheap and biologically plausible machine learning (ML) scheme, based on the combination (ensemble learning) of simple linear classifiers. Our learning architecture can be thought as a combination of hardware-based reservoir computing systems,[10–12] where different reservoirs are given by outputs of our photonic ANN at different wavelengths. In particular, we show that the classification accuracy of handwritten digits steadily increases by employing more and more nonlinear representations from our photonic ANN, and that

Further author information: (Send correspondence to A.L.)
A.L.: E-mail: alessio.lugnan.1@unitn.it

it significantly overcomes the accuracy obtained substituting the nonlinear representations with linear ones, demonstrating the key role of the proposed neuromorphic hardware.

This work is inspired by a previous research[13] and presents, in comparison, few important improvements. In particular, here we employ a more energy efficient photonic ANN, as it does not include phase change materials for reconfigurability and it presents a better connected topology. Moreover, in this work we employ an improved ML scheme and we use the full MNIST dataset without any preprocessing. Finally, the acquisition of the images processed by our photonic ANN is self-triggered and therefore does not need any synchronization with the input signal, e.g. by means of an external clock signal.

2. RESULTS

We inserted flattened MNIST images (70000 images) in our integrated photonic ANN by modulating infrared laser light (wavelengths around 1550 nm, see Fig. 1 a) with a sampling time of 2 ns. Peak optical powers of few mW allowed us to trigger strong nonlinear dynamics in the MRRs network, linked to two-photon absorption in silicon and based on variations of free carriers density and temperature in the MRRs.[14] In particular, free carriers provide nonlinear short-term memory with a characteristic time of few nanoseconds, while temperature provides nonlinear long-term memory with a characteristic time of few hundred nanoseconds. The input insertion was repeated for 11 different laser wavelengths (approximating concurrent parallel insertion), each providing a different time-dependent representation acquired at output port 2 (see Fig. 1 a). Specifically, the employed wavelengths (in nanometers) are 1556.55, 1555.91, 1555.75 , 1555.59, 1555.42, 1555.26, 1555.10, 1554.94, 1554.78, 1554.62, 1554.46, 1556.55. The first wavelength was chosen so that it did not excite any MRR resonance, resulting in a linear representation of the input to be used as a reference and to obtain a ML baseline. The other wavelengths excited different MRR resonances, resulting into different nonlinear representations at the output ports. Moreover, for each resonant wavelength, 10 optical different power levels were considered, each providing different nonlinear representations as well. Namely, the estimated on-chip power levels were (respectively mean and peak power in milliwatt): 0.086, 0.17, 0.26, 0.34, 0.43, 0.51, 0.60, 0.69., 0.77, 0.86, and 1.5, 3.0, 4.5, 6.1, 7.6, 9.1, 10.6, 12.2, 13.7, 15.2. For the (first) non-resonant wavelength we only employed the higher power level among the listed ones. Therefore, we measured a total of 101 different output representations of the input, all at the same output port.

Regarding the ML analysis, we separated the first 60000 samples from the subsequent 10000, respectively employed as training and test sets. The first step of our training procedure consists of training a linear classifier (logistic regression) using 10000 samples of the training set, where the employed features came from the linear output representation (i.e. with the non-resonant wavelength of 1556.55 nm). In the second step, we select the best nonlinear representation to be combined with the system trained in the first step, among the ones obtained using the first resonant wavelength (namely 1556.55 nm) and different power levels. In particular, for each power level we trained a linear classifier using 14500 samples of the training set, employing as features the corresponding nonlinear representation together with the output of the previously trained linear classifier (see Fig. 1 b). We evaluated its performance using the rest of the training set (here employed as a validation set). Afterwards we selected the case giving the best validation accuracy. The third step of our training procedure is a repetition of the second: considering the second resonant wavelength and for each input power level, we train a linear classifier using 19000 training samples, employing as features the current nonlinear representation together with the outputs of the 2 previously trained and chosen classifiers. Again, we employ the rest of the training set to evaluate and choose the best power level for the given wavelength. These steps are repeated until all the 10 resonant wavelength have been considered. Moreover, in order to evaluate how much of the classification accuracy is due to the nonlinear representations produced by our neuromorphic hardware, we repeated the training procedure employing only the linear representation generated using the non-resonant wavelength. Overall, each step of this training procedure is meant to progressively improve the performance of the whole model, by learning how to correct the mistakes made in the previous steps.

The final ML accuracy was estimated by evaluating each trained linear classifier on the test dataset (last 10000 MNIST images), each one corresponding to a different number of chosen nonlinear representations (see Fig. 1 c). We notice that the classification performance steadily increases with the number of employed nonlinear representations, and that it is significantly greater than the linear baseline. These results show that our photonic

ANN can be used to enhance the ML performance obtainable with simple and computationally cheap linear classifiers. Importantly, the full ML model is biologically plausible and does not require observation and control of the internal states and parameters of the neuromorphic hardware. Moreover, it should be stressed that many more different nonlinear representations can be obtained from our photonic ANN (e.g., by employing different output ports) and that the network could be easily scaled up to significantly larger number of neurons (MRRs) and input/output ports.

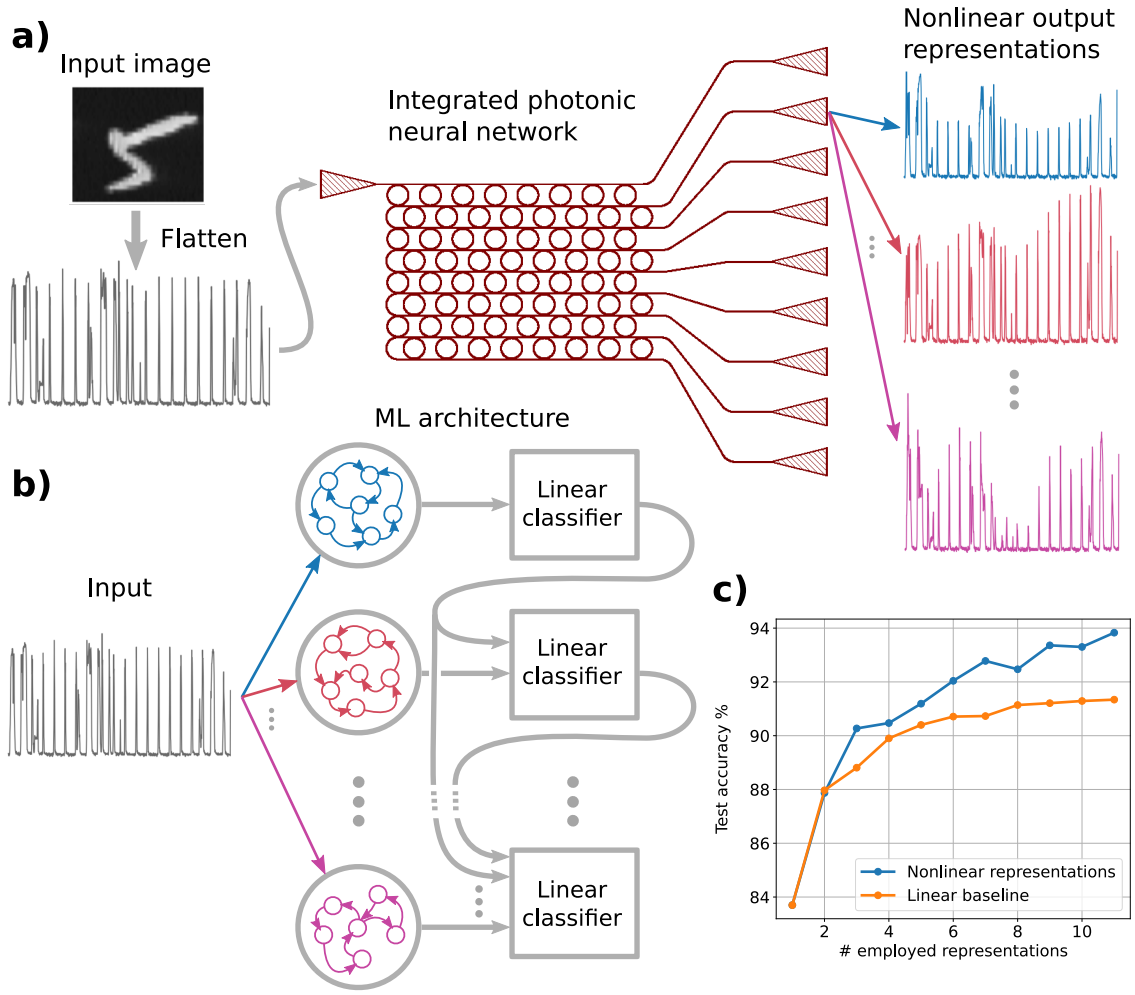

Figure 1. ML classification of handwritten digits enhanced by an integrated photonic ANN. **a)** Images are flattened and inserted as an optical time series into our MRR network, which produces several nonlinear representations of the input, depending on the output physical port, the laser wavelength and power. **b)** Diagram of the employed ML model. The input signal is inserted into different recurrent networks (each representing the nonlinear transformation performed by our photonic ANN at different input wavelength). The output of the first is used to train a linear classifier, whose output is joined to the output of the second recurrent network and used to train the second linear classifier, and so on. This way, each linear classifier is trained to improve on the previous one, exploiting different nonlinear representations of the input. **c)** Classification accuracy of the different employed linear classifiers (blue), corresponding to different numbers of exploited nonlinear representations. This is compared with the accuracy of the same ML model (orange) where only linear representations are used.

3. CONCLUSION

In this work we propose a novel integrated photonic neural network based on coupled silicon microring resonators. This neuromorphic hardware can host complex nonlinear dynamics and is able to produce several different nonlinear representations of its input, via highly parallel operations in the spatial, temporal and frequency domains. We showed that, even employing only a single physical output port, our photonic ANN could generate 100 different nonlinear representations of its input signal (flattened images of handwritten digits, namely the MNIST dataset), by varying the input laser wavelength and power. Moreover, we demonstrated a biologically plausible and computationally cheap machine learning scheme that could exploit these nonlinear representations in order to significantly increase its accuracy in image classification (MNIST task). As a next step, we aim to investigate the exploitation of multiple physical output ports, e.g. integrating an automatic exploration and optimization of the generated representations directly into the measurement process, thus limiting the data to be measured and stored. Furthermore, we plan to test our neuromorphic system and machine learning scheme on other tasks, such as fashion MNIST and time series prediction.

ACKNOWLEDGMENTS

This work was funded by the European Union's Horizon 2020 and Horizon Europe Research and Innovation Programmes (grant 780848 Fun-COMP, grant 101070238 NEUROPULS and grant 101064322 ARIADNE).

REFERENCES

[1] Xu, M., Chen, X., Guo, Y., Wang, Y., Qiu, D., Du, X., Cui, Y., Wang, X., and Xiong, J., "Reconfigurable neuromorphic computing: Materials, devices and integration," *Advanced Materials* , 2301063 (2023).

[2] Shastri, B. J., Tait, A. N., Ferreira de Lima, T., Pernice, W. H., Bhaskaran, H., Wright, C. D., and Prucnal, P. R., "Photonics for artificial intelligence and neuromorphic computing," *Nature Photonics* **15**(2), 102–114 (2021).

[3] Pavanello, F., Vatajelu, E. I., Bosio, A., Van Vaerenbergh, T., Bienstman, P., Charbonnier, B., Carpegna, A., Di Carlo, S., and Savino, A., "Special session: Neuromorphic hardware design and reliability from traditional cmos to emerging technologies," in [*2023 IEEE 41st VLSI Test Symposium (VTS)*], 1–10, IEEE (2023).

[4] Schmidgall, S., Achterberg, J., Miconi, T., Kirsch, L., Ziaei, R., Hajiseyedrazi, S., and Eshraghian, J., "Brain-inspired learning in artificial neural networks: a review," *arXiv preprint arXiv:2305.11252* (2023).

[5] Lillicrap, T. P., Santoro, A., Marris, L., Akerman, C. J., and Hinton, G., "Backpropagation and the brain," *Nature Reviews Neuroscience* **21**(6), 335–346 (2020).

[6] Bogaerts, W., De Heyn, P., Van Vaerenbergh, T., De Vos, K., Kumar Selvaraja, S., Claes, T., Dumon, P., Bienstman, P., Van Thourhout, D., and Baets, R., "Silicon microring resonators," *Laser & Photonics Reviews* **6**(1), 47–73 (2012).

[7] Mancinelli, M., Borghi, M., Ramiro-Manzano, F., Fedeli, J., and Pavesi, L., "Chaotic dynamics in coupled resonator sequences," *Optics express* **22**(12), 14505–14516 (2014).

[8] Biasi, S., Donati, G., Lugnan, A., Mancinelli, M., Staffoli, E., and Pavesi, L., "Photonic neural networks based on integrated silicon microresonators," *Intelligent Computing* **3**, 0067 (2024).

[9] LeCun, Y. and Cortes, C., "MNIST handwritten digit database." http://yann.lecun.com/exdb/mnist/ (2010).

[10] Tanaka, G., Yamane, T., Héroux, J. B., Nakane, R., Kanazawa, N., Takeda, S., Numata, H., Nakano, D., and Hirose, A., "Recent advances in physical reservoir computing: A review," *Neural Networks* **115**, 100–123 (2019).

[11] Lugnan, A., Katumba, A., Laporte, F., Freiberger, M., Sackesyn, S., Ma, C., Gooskens, E., Dambre, J., and Bienstman, P., "Photonic neuromorphic information processing and reservoir computing," *APL Photonics* **5**(2) (2020).

[12] Freiberger, M., Sackesyn, S., Ma, C., Katumba, A., Bienstman, P., and Dambre, J., "Improving time series recognition and prediction with networks and ensembles of passive photonic reservoirs," *IEEE Journal of Selected Topics in Quantum Electronics* **26**(1), 1–11 (2019).

[13] Lugnan, A., Aggarwal, S., Brückerhoff-Plückelmann, F., Wright, C. D., Pernice, W. H., Bhaskaran, H., and Bienstman, P., "Emergent self-adaptation in an integrated photonic neural network for backpropagation-free learning," *arXiv preprint arXiv:2312.03802* (2023).

[14] Van Vaerenbergh, T., Fiers, M., Mechet, P., Spuesens, T., Kumar, R., Morthier, G., Schrauwen, B., Dambre, J., and Bienstman, P., "Cascadable excitability in microrings," *Optics express* **20**(18), 20292–20308 (2012).